Journal of ELECTRONIC MATERIALS, Vol. 42, No. 6, 2013
DOI: 10.1007/s11664-012-2464-0

Effect of Sintering Temperature on Microstructure, Electrical Properties, and Thermal Expansion of Perovskite-Type $La_{0.8}Ca_{0.2}CrO_3$ Complex Oxides Synthesized by a Combustion Method

WENFENG GUO,[1,2,4] YINGZI WANG,[3] ADAN LI,[1] TIFENG JIAO,[1] and FAMING GAO[1]

1.—Hebei Key Laboratory of Applied Chemistry, School of Environmental and Chemical Engineering, Yanshan University, Qinhuangdao 066004, China. 2.—State Key Laboratory of Metastable Materials Science and Technology, Yanshan University, Qinhuangdao 066004, China. 3.—School of Material Science and Engineering, University of Jinan, Jinan 250022, China. 4.—e-mail: wfguo@ysu.edu.cn

Perovskite-type $La_{0.8}Ca_{0.2}CrO_3$ complex oxides were synthesized by a combustion method. Microstructural evolution, electrical properties, and thermal expansion behavior of the ceramics were investigated in the sintering temperature range of 1250°C to 1450°C. It was found that the electrical conductivity (σ_e) remarkably improved with increasing sintering temperature from 1250°C to 1400°C, ascribed to the development of microstructural densification, whereas it declined slightly above 1400°C due to generation of excessive liquid. The specimen sintered at 1400°C had a maximum conductivity of 31.6 S cm^{-1} at 800°C, and lowest activation energy of 0.148 eV. The improvement of the thermal expansion coefficient (TEC) with increasing sintering temperature was monotonic as a result of the microstructural densification of the materials. The TEC of $La_{0.8}Ca_{0.2}CrO_3$ sintered at 1400°C was about 10.5×10^{-6} K^{-1}, being consistent with other components as high-temperature conductors. With respect to microstructure, electrical properties, and thermal expansion, the preferable sintering temperature was ascertained to be about 1400°C, which is much lower than for the traditional solid-state reaction method.

Key words: $La_{0.8}Ca_{0.2}CrO_3$, microstructure, electrical conductivity, activation energy, thermal expansion coefficient (TEC)

INTRODUCTION

Perovskite-type complex oxides of doped lanthanum chromites are attracting increasing attention as high-temperature conductors because of their superior electronic conductivity and excellent chemical stability in both oxidizing and reducing atmospheres. These preeminent characteristics make them promising candidate materials for many important applications, such as interconnectors for solid-oxide fuel cells (SOFC), heating elements for high-temperature furnaces, and current-collecting electrodes in magnetohydrodynamics (MHD).[1–4] However, their applications are limited by poor sinterability, due to appreciable volatilization loss of chromium oxide at high temperatures in oxidizing atmosphere.[5] Therefore, a considerable amount of research effort has been applied to improving the sinterability of doped lanthanum chromites, and it was found that alkaline-earth doping, especially Ca doping, provided reasonably optimum properties.[6–8]

The combustion method, as a wet chemical method, is accompanied by the release of a relatively large

(Received November 19, 2012; accepted December 28, 2012; published online February 28, 2013)

amount of heat and gases, which facilitates rapid formation of unagglomerated, highly reactive powders and can enhance the sinterability of doped lanthanum chromites.[9,10] In this work, we synthesized $La_{0.8}Ca_{0.2}CrO_3$ powders by a combustion method using metal nitrates as oxidizers and glycine as fuel, and the resulting powders were pressed and sintered to create dense ceramics. The effects of sintering temperature on microstructure, electrical properties, and thermal expansion of the ceramics were investigated. The objective of this work is to identify the optimum sintering temperature to achieve a phase-pure fully densified ceramic.

EXPERIMENTAL PROCEDURES

$La_{0.8}Ca_{0.2}CrO_3$ powders were synthesized by a combustion method. Reagent-grade $La(NO_3)_3{\cdot}6H_2O$, $Ca(NO_3)_2{\cdot}4H_2O$, $Cr(NO_3)_3{\cdot}9H_2O$, and glycine were used as starting materials. The nitrates were weighed according to the nominal composition $La_{0.8}Ca_{0.2}CrO_3$, then dissolved into deionized water in a beaker. A designed amount of glycine was added, with a molar ratio of glycine to total metal cation of 2:1. The mixture was heated and concentrated up to combustion to form the primary powders. The primary powders were pulverized and calcined at 600°C for 1 h. Good perovskite structure, in association with a tiny amount of $CaCrO_4$ as a temporary phase enhancing sintering,[11–14] was identified for the calcined powder by x-ray diffraction (XRD, Rigaku D/MAX-RB x-ray diffractometer). Scanning electron microscopy (SEM, Jeol JMS-5610LV) analysis showed that the powders consisted of homogeneous particles with a main size distribution of ~100 nm. The fine powders were uniaxially pressed into rectangular bars (30 mm × 4 mm × 4 mm) and disks (Φ13 mm × 2 mm), followed by sintering at 1250°C to 1450°C for 4 h in air.

Relative densities of the sintered specimens were determined from the apparent density values measured by the Archimedes method and the theoretical density calculated from the lattice parameter of the solid solution. After etching in diluted hybrid acids, fractured cross-sections of sintered specimens were investigated by SEM. The ceramic specimens were polished to ensure surface flatness. The rectangular specimens were painted with platinum paste for measurement of electrical conductivity. The electrical conductivity was then measured at 25°C to 800°C by a direct-current (dc) four-terminal method in air. Thermal expansion measurements were conducted using a dilatometer (NETZSCH DIL 402C) at a heating rate of 5°C min^{-1} from room temperature to 800°C in air.

RESULTS AND DISCUSSION

Figure 1 shows the linear shrinkage and relative density of $La_{0.8}Ca_{0.2}CrO_3$ sintered at various temperatures for 4 h in air. The disk specimens were made from powders synthesized by the combustion method. The linear shrinkage of the specimens increased gradually from 14.3% to 16.3% with the sintering temperature in the range from 1250°C to 1400°C. When the sintering temperature was increased further, the shrinkage exhibited almost no change, implying that the $La_{0.8}Ca_{0.2}CrO_3$ specimens became sufficiently close-grained at 1400°C.

The relative density was tested to assess the density achieved by sintering the disks. As observed in Fig. 1, there was a considerable increase of relative density from 78.2% to 96.5% with elevation of the sintering temperature from 1250°C to 1450°C. It can be seen that this increase mostly happened in the sintering temperature range from 1250°C to 1400°C. When sintered at temperature of 1400°C, the relative density already reached 94.9%, an adequate value. After 1400°C, the relative densities of the specimens tended to plateau. This is consistent with the linear shrinkage results.

Figure 2 shows SEM micrographs of fracture surfaces of $La_{0.8}Ca_{0.2}CrO_3$ sintered at different temperatures for 4 h in air. The specimens were prepared by the combustion method. A porous microstructure with small grain size was observed in the specimen sintered at 1300°C. Increase of the sintering temperature significantly promoted grain growth and microstructural densification. Compared with the microstructure at 1300°C and 1350°C, there was obvious grain growth and density increase in the specimens sintered at 1400°C and 1450°C, respectively.

The increases of the relative density and linear shrinkage reflect the microstructural evolution. The above results indicate that an adequate sintering temperature for $La_{0.8}Ca_{0.2}CrO_3$ ceramic was about 1400°C. It is well known that the chromium component, in the form of chromium oxides, can volatilize and deposit on the particle surface, without particle contact and growth, when sintered at high temperatures in air. This leads to a sintering

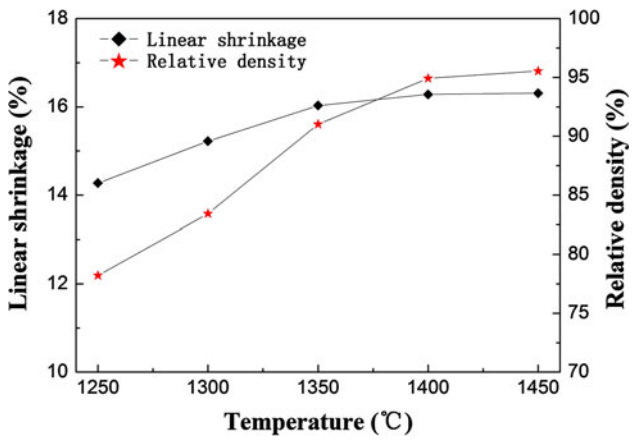

Fig. 1. Relative density of $La_{0.8}Ca_{0.2}CrO_3$ ceramics sintered at various temperatures.

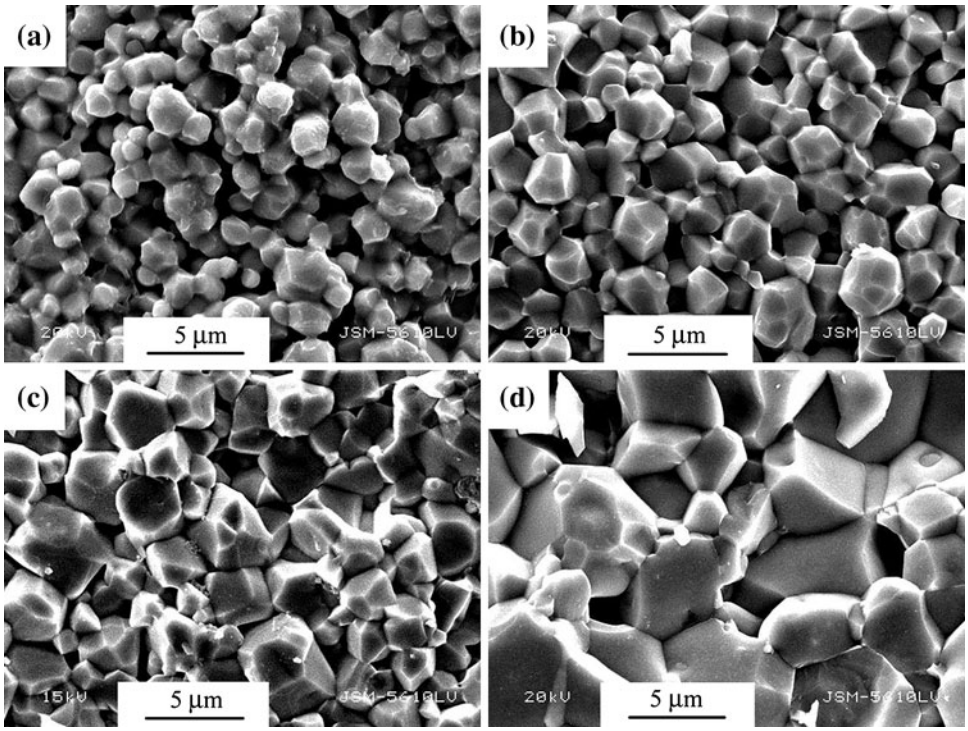

Fig. 2. SEM micrographs of fracture surfaces of $La_{0.8}Ca_{0.2}CrO_3$ ceramics sintered at (a) 1300°C, (b) 1350°C, (c) 1400°C, and (d) 1450°C.

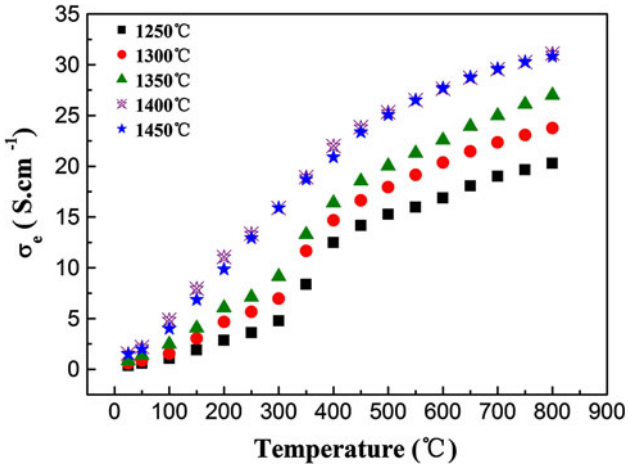

Fig. 3. Electrical conductivity (σ_e) of $La_{0.8}Ca_{0.2}CrO_3$ ceramics sintered at different temperatures as a function of measuring temperature.

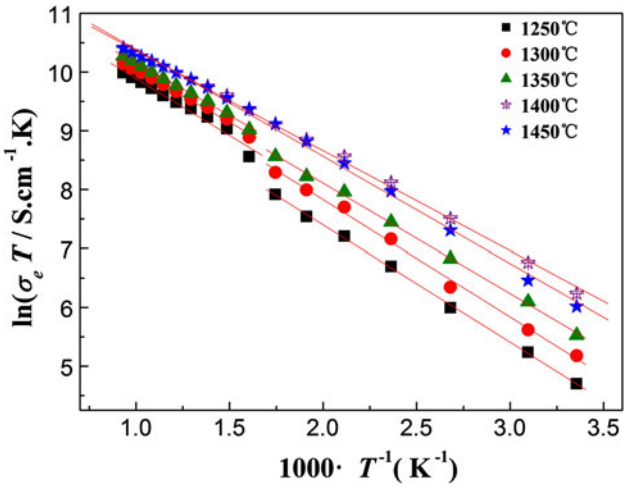

Fig. 4. Plots of $\ln(\sigma_e T)$ versus $1000/T$ for $La_{0.8}Ca_{0.2}CrO_3$ ceramics sintered at different temperatures.

mechanism with neck growth but no densification for lanthanum chromite.[13–15] However, in the present work, we believe that the highly reactive fine powders promoted mass transport at a lower temperature, avoiding chromium loss. Thus, highly dense material could be achieved at sintering temperature as low as 1400°C. Therefore, the combustion method can effectively enhance the sinterability of the material and decrease the sintering temperature required to obtain dense lanthanum chromite.

Figure 3 shows the electrical conductivity σ_e of $La_{0.8}Ca_{0.2}CrO_3$ ceramics as a function of measuring temperature. The specimens were prepared by the combustion method and sintered at different temperatures for 4 h in air. With increase of the sintering temperature from 1250°C to 1400°C, the electrical conductivities of the different sintered specimens improved remarkably. Further increase of the sintering temperature above 1400°C decreased the electrical conductivity slightly. The

specimen sintered at 1400°C had maximum conductivity of 31.6 S cm^{-1} at 800°C, approximating results (~30 S cm^{-1}) in the literature.[16] Together with the microstructure, this can possibly be ascribed to two factors: the development of densification, and the generation of liquid. Elevation of the density promotes electronic conduction, but excessive liquid with abnormally large grains blocks transport of electronic carriers at too high a temperature.

In addition, it is worth noting that the electrical conductivities of the specimens sintered in the range of 1250°C to 1350°C displayed an uneven change with increasing measuring temperature, with a sharp rise of electrical conductivity between 300°C and 400°C. This might be attributable to a porous microstructure with small grain size, which prevented carrier transfer below 300°C, while above 400°C a lower activation energy was gained in virtue of lattice vibrations. Accordingly, the results are also presented in Fig. 4 as plots of log $\sigma_e T$ versus $1000/T$ for the specimens (where T is the absolute temperature). The plots of the specimens sintered at 1250°C to 1350°C consist of two line segments, whereas the plots above 1400°C are nearly single lines.

Both the single line and the plots with two line segments suggest that small polaron hopping is the predominant mechanism for electronic conduction, as expressed by the following equation:[12,17,18]

$$\sigma_e = (C/T)\exp(-E_a/kT),$$

where C is a material constant containing the carrier concentration term, E_a is the activation energy for small polaron hopping, and k is the Boltzmann constant. According to Fig. 4, E_a was calculated from linear fits to the plots over the different temperature ranges and is presented in Table I. It can be seen that, in the sintering temperature range of 1250°C to 1450°C, the E_a of $La_{0.8}Ca_{0.2}CrO_3$ sintered at 1400°C reached its lowest value of 0.148 eV.

Figure 5 shows the thermal expansion behavior of $La_{0.8}Ca_{0.2}CrO_3$ ceramics sintered at different temperatures for 4 h in air. The specimens were prepared by the combustion method. It was found that the relative expansion ($\Delta L/L$) of the diverse specimens evidently improved with increasing sintering temperature up to 1400°C, albeit with a slight change after 1400°C. The variation of the thermal expansion behavior with increasing sintering temperature is consistent with the relative density results due to the development of microstructure and densification. Besides, a kink appears in the relative expansion plots between 300°C and 450°C, probably due to the orthorhombic-to-rhombohedral phase transition.[18,19]

The thermal expansion coefficient (TEC) of $La_{0.8}Ca_{0.2}CrO_3$ was measured for different sintering temperatures and is presented in Table II. As is well known, high-temperature conductors, such as interconnects and electrodes, operate at high temperatures and should endure thermal cycling from room temperature to the operating temperature. Therefore, they have to be thermally compatible with other components to minimize thermal stresses. The TEC of $La_{0.8}Ca_{0.2}CrO_3$ sintered at 1400°C was about 10.5×10^{-6} K^{-1} in the temperature range from 30°C to 800°C in air, being accordant with that of other high-temperature components, such as yttria-stabilized zirconia electrolyte (~10.5×10^{-6} K^{-1}) for use in SOFCs.

It is notable that the microstructural evolution with sintering temperature corresponds well to the variation of the electrical conductivity and TEC of $La_{0.8}Ca_{0.2}CrO_3$ ceramic. Based on the presented

Table IE$_a$ of $La_{0.8}Ca_{0.2}CrO_3$ ceramics sintered at different temperatures

Sintering Temperature (°C)	1250	1300	1350	1400	1450
E_a (eV)	0.171[a] 0.167[b]	0.168[a] 0.155[b]	0.169[a] 0.155[b]	0.148	0.157

[a]Low-temperature region (25°C to 300°C)[b]High-temperature region (400°C to 800°C).

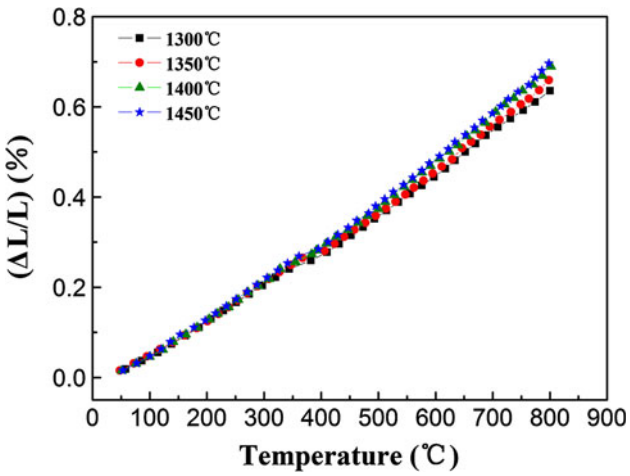

Fig. 5. Thermal expansion behavior of $La_{0.8}Ca_{0.2}CrO_3$ ceramics sintered at different temperatures.

Table II. Thermal expansion coefficient of $La_{0.8}Ca_{0.2}CrO_3$ ceramics sintered at different temperatures

T (°C)	1300	1350	1400	1450
α (10^{-6} K^{-1})	8.5[a] 9.7[b]	8.6[a] 10.2[b]	8.8[a] 10.5[b]	8.9[a] 10.7[b]

[a]Low-temperature region (25°C to 300°C)[b]High-temperature region (450°C to 800°C).

results, it was ascertained that the ceramic could be densely sintered at 1400°C. In contrast, ceramic samples made by the solid-state reaction method require a much higher sintering temperature (above 1550°C) to obtain the same level of compaction.[20] Apparently, the combustion method could effectively decrease the sintering temperature of $La_{0.8}Ca_{0.2}CrO_3$.

CONCLUSIONS

The combustion method was confirmed to be an advantageous process for synthesis of perovskite-type $La_{0.8}Ca_{0.2}CrO_3$ complex oxides. With respect to microstructure, electrical properties, and thermal expansion, the preferable sintering temperature of the ceramic specimens prepared by the combustion method was ascertained to be about 1400°C, which is much lower than for the traditional solid-state reaction method. This makes the combustion method attractive for industrial manufacturing of ceramic components from lanthanum chromites.

ACKNOWLEDGEMENTS

This project was financially supported by the Scientific and Technological Research and Development Program of Hebei Province (Grant No. 11215171), the Science & Technology Pillar Program of Hebei Province (Grant No. 11276736), the China Postdoctoral Science Foundation (Grant No. 2011M500540), and the Scientific Research Foundation for Returned Overseas Chinese Scholars of Hebei Province (Grant No. 2011052).

REFERENCES

1. W. Faduska and A.O. Isenberg, *J. Power Sources* 10, 89 (1983).
2. N.Q. Minh, *J. Am. Ceram. Soc.* 76, 563 (1993).
3. S.P.S. Badwal, *Solid State Ionics* 143, 39 (2001).
4. I. Yasuda and T. Hikita, *J. Electrochem. Soc.* 140, 1699 (1993).
5. L. Groupp and H.U. Adersen, *J. Am. Ceram. Soc.* 59, 449 (1976).
6. M.M. Rashad and S.M. El-Sheikh, *Mater. Res. Bull.* 46, 469 (2011).
7. S.R. Nair, R.D. Purohit, A.K. Tyagi, P.K. Sinha, and B.P. Sharma, *Mater. Res. Bull.* 43, 1573 (2008).
8. F. Deganello, G. Marcì and G. Deganello, *J. Eur. Ceram.* Soc. 29, 439 (2009).
9. L.A. Chick, L.R. Pederson, G.D. Maupin, and J.L. Bates, *Mater. Lett.* 10, 6 (1990).
10. S.M. Alexander, C. Colleen, P.S. Katherine, L. David, and V. Arvind, *Sep. Purif. Technol.* 25, 117 (2001).
11. L.A. Chick, J. Liu, J.W. Stevenson, T.R. Armstrong, D.E. McCready, G.D. Maupin, G.W. Coffey, and C.A. Coyle, *J. Am. Ceram. Soc.* 80, 2109 (1997).
12. T.R. Armstrong, J.W. Stevenson, K. Hansinska, and D.E. McCready, *J. Electrochem. Soc.* 145, 4282 (1998).
13. A. Chakraborty, R.N. Basu, and H.S. Maiti, *Mater. Lett.* 45, 162 (2000).
14. S.L. Wang, B. Lin, K. Xie, Y.C. Dong, X.Q. Liu, and G.Y. Meng, *J. Alloy. Compd.* 468, 499 (2009).
15. J.W. Stevenson, P.F. Hallman, T.R. Armstrong, and L.A. Chick, *J. Am. Ceram. Soc.* 78, 507 (1995).
16. S.H. Pi, S.B. Lee, R.H. Song, J.W. Lee, T.H. Lim, S.J. Park, D.R. Shin, and C.O. Park, *Int. J. Hydrogen Energ.* 36, 13735 (2011).
17. H. Xiong, G.J. Zhang, and J.Y. Zheng, *Mater. Lett.* 51, 61 (2001).
18. H. Hayashi, M. Watanabe, M. Ohuchida, H. Inaba, Y. Hiei, T. Yamamoto, and M. Mori, *Solid State Ionics* 144, 301 (2001).
19. N. Sakai, H. Fjellvåg, and B.C. Hauback, *J. Solid State Chem.* 121, 202 (1996).
20. R.K. Gupta and C.M. Whang, *Solid State Ionics* 178, 1617 (2007).